JOC*Article*

Diphenylnitrenium Ion: Cyclization, Electron Transfer, and Polymerization Reactions

Andrew C. Kung, Sean P. McIlroy, and Daniel E. Falvey*

Department of Chemistry and Biochemistry, University of Maryland, College Park, Maryland 20742-2021

falvey@umd.edu

Received March 24, 2005

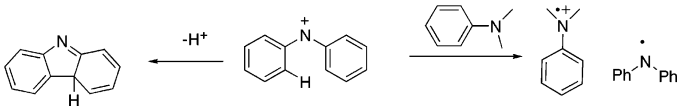

Reactions of diphenylnitrenium ion were examined using laser flash photolysis (LFP), product analysis, and computational modeling using density functional theory (DFT). In the absence of trapping agents, diphenylnitrenium ion cyclizes to form carbazole. On the basis of laser flash photolysis experiments and DFT calculations it is argued that this process is a concerted cyclization/proton transfer that forms the H-4a tautomer of carbazole. Additional LFP experiments and product studies show that diphenylnitrenium ion reacts with electron-rich arenes (e.g., *N*,*N*-dimethylaniline, diphenylamine, and carbazole) through an initial one-electron transfer. The radical intermediates formed in this step then couple to form dimeric products. Secondary reactions between the diphenylnitrenium ion and these dimers results in the formation of oligomeric materials.

Introduction

Nitrenium ions are highly reactive transient species that contain a positively charged and dicoordinate nitrogen atom.[1−3] These short-lived intermediates are of interest due to their involvement in carcinogenic DNA-damaging reactions[4−7] and their postulated involvement in the synthesis of polyaniline (PANI).[8] There is also some recent interest in using these species in synthetic chemistry.[9−11] The development of methods for directly detecting nitrenium ions using fast laser methods resulted in a recent increase in interest in these species.[12−14] The present report concerns the reactions of *N*,*N*-diphenylnitrenium ion (**1**). Previous studies using chemical trapping[14,15] laser flash photolysis (LFP),[16] time-resolved infrared spectroscopy,[17] and time-resolved Raman spectroscopy[18] have established that this species is generated upon photolysis of 1-(*N*,*N*-diphenylamino)-2,4,6-trimethylpyridinium ions (**2**), as shown in Scheme 1. It was also shown that Ph_2N^+, like most simple aromatic nitrenium ions,[19−24] is a ground-state singlet.[15,25] Its known decay

* To whom correspondence should be addressed. Fax: 301-314-9121.

(1) Abramovitch, R. A.; Jeyaraman, R. Nitrenium Ions. In *Azides and Nitrenes: Reactivity and Utility*; Scriven, E. F. V., Ed.; Academic: Orlando, FL, 1984; pp 297−357.

(2) Falvey, D. E. Nitrenium Ions. In *Reactive Intermediate Chemistry*; Moss, R. A., Platz, M. S., Maitland Jones, J., Eds.; Wiley-Interscience: Hoboken, NJ, 2004; Vol. 1; pp 593−650.

(3) Novak, M.; Rajagopal, S. *Adv. Phys. Org. Chem.* **2001**, *36*, 167−254.

(4) Famulok, M.; Bosold, F.; Boche, G. *Angew. Chem., Int. Ed. Engl.* **1989**, *28*, 337−338.

(5) Kadlubar, F. F. DNA Adducts of Carcinogenic Amines. In *DNA Adducts Identification and Biological Significance*; Hemmink, K., Dipple, A., Shuker, D. E. G., Kadlubar, F. F., Segerbäck, D., Bartsch, H., Eds.; University Press: Oxford, UK, 1994; pp 199−216.

(6) Hoffman, G. R.; Fuchs, R. P. P. *Chem. Res. Toxicol.* **1997**, *10*, 347−359.

(7) Novak, M.; Kazerani, S. *J. Am. Chem. Soc.* **2000**, *122*, 3606−3616.

(8) Wei, Y.; Jang, G.-W.; Chan, C. C.; Hsueh, K. F.; Hariharan, R.; Patel, S.; Whitecar, C. K. *J. Phys. Chem.* **1990**, *94*, 7716−7721.

(9) Rodrigues, J. A. R.; Abramovitch, R. A.; de Sousa, J. D. F.; Leiva, G. *J. Org. Chem.* **2004**, *69*, 2920−2928.

(10) Wardrop, D. J.; Zhang, W. *Org. Lett.* **2001**, *3*, 2353−2356.

(11) Wardrop, D. J.; Birge, M. S. *Chem. Commun.* **2004**, 1230−1231.

(12) Anderson, G. B.; Falvey, D. E. *J. Am. Chem. Soc.* **1993**, *115*, 9870−9871.

(13) McClelland, R. A. *Tetrahedron* **1996**, *52*, 6823−6858.

(14) Moran, R. J.; Falvey, D. E. *J. Am. Chem. Soc.* **1996**, *118*, 8965−8966.

(15) Moran, R. J.; Cramer, C. J.; Falvey, D. E. *J. Org. Chem.* **1996**, *61*, 3195−3199.

(16) McIlroy, S.; Moran, R. J.; Falvey, D. E. *J. Phys. Chem. A* **2000**, *104*, 11154−11158.

(17) Srivastava, S.; Toscano, J. P.; Moran, R. J.; Falvey, D. E. *J. Am. Chem. Soc.* **1997**, *119*, 11552−11553.

(18) Zhu, P.; Ong, S. Y.; Chan, P. Y.; Poon, Y. F.; Leung, K. H.; Phillips, D. L. *Chem. Eur. J.* **2001**, *7*, 4928−4936.

(19) Cramer, C. J.; Dulles, F. J.; Falvey, D. E. *J. Am. Chem. Soc.* **1994**, *116*, 9787−9788.

(20) Sullivan, M. B.; Brown, K.; Cramer, C. J.; Truhlar, D. G. *J. Am. Chem. Soc.* **1998**, *120*, 11778−11783.

(21) McIlroy, S.; Cramer, C. J.; Falvey, D. E. *Org. Lett.* **2000**, *2*, 2451−2454.

(22) Ford, G. P.; Herman, P. S. *J. Am. Chem. Soc.* **1989**, *111*, 3987−3996.

(23) Li, Y.; Abramovitch, R. A.; Houk, K. N. *J. Org. Chem.* **1989**, *54*, 2911−2914.

(24) Falvey, D. E.; Cramer, C. J. *Tetrahedron Lett.* **1992**, *33*, 1705−1708.

10.1021/jo050598z CCC: $30.25
Published on Web 05/26/2005

SCHEME 1. Decay Pathways for Diphenylnitrenium Ion (1)

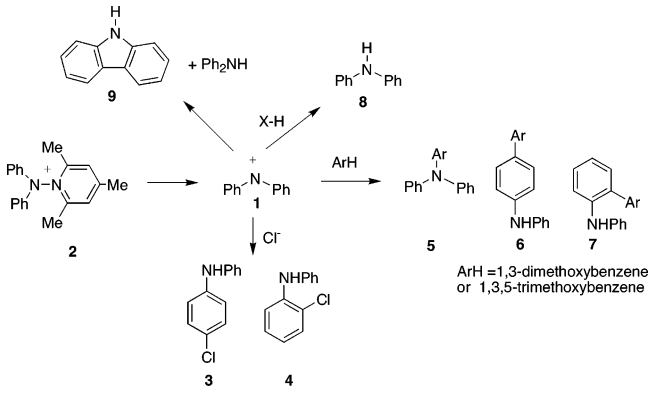

reactions include (1) addition of simple nucleophiles (e.g., halides, alcohols) to the *ortho* and *para* positions on the phenyl rings,[14,15,17] (2) addition of electron-rich aromatic compounds (e.g., 1,3,5-trimethoxybenzene) to the nitrenium nitrogen atom via a σ complex intermediate,[26] and (3) abstraction of hydride from a suitable donor (e.g., 1,4-cyclohexadiene).[16] These reaction pathways are summarized in Scheme 1.

When diphenylnitrenium ion (**1**) is generated in the absence of trapping agents, stable products include diphenylamine (**8**) and carbazole (**9**), which are formed in relatively low yields.[14] Along with these two products, large amounts of colored materials were formed. The latter had not been characterized, but they were presumed to be high molecular weight oligomers related to poly(diphenylamine).

The present study was undertaken with three goals. First, we wanted to elucidate the primary decay pathway for diphenylnitrenium ion in the absence of traps. It was not clear at the outset of this study whether the formation of diphenylamine and the other products occurred concurrently with the carbazole pathway or resulted from secondary decay reactions. Through a combination of LFP, product analysis, and computational modeling, we provide evidence that cyclization is the primary decay pathway and that the other products result from secondary reactions.

A second goal was to determine the nature of the uncharacterized colored materials as well as the mechanism of their formation. Obviously, this serves the first goal by differentiating primary and secondary decay processes. Increasing commercial importance of PANI and its derivatives also encouraged us to examine this process. Formation of poly(diphenylamine) in these reactions may provide additional insight into the possible involvement of nitrenium ions in PANI synthesis, as well as to help identify new methods by which these important polymers could be prepared. Below, we demonstrate by MALDI-TOF-MS that polymers are formed in these reactions and LFP experiments provide some insights into the mechanism by which this occurs.

The third goal was to determine the mechanism by which diphenylnitrenium ion reacts with electron-rich aromatic compounds. This was occasioned by our interest in the polymerization mechanism, but it is also relevant to newly emerging synthetic applications of nitrenium ion chemistry and to the issue of DNA damage by nitrenium ions. Our LPF and product studies indicate that with easily oxidized arenes, the reaction with the nitrenium ion can proceed through an initial electron transfer, followed by coupling to yield dimeric adducts.

TABLE 1. Yields of 8 and 9 from Photolysis of Various Initial Concentrations of 2 in Various Solvents

solvent	concn of **2** (mM)	**8** (%)	**9** (%)
$PhCH_3$	0.097	26	27
$PhCH_3$	4.6	35	10
CH_3CN	0.097	10	67
CH_3CN	0.34	7	22
CH_3CN	4.5	5	36
CH_2Cl_2	0.064	26	36
CH_2Cl_2	4.85	54	1.4

Results and Discussion

A. Carbazole Formation. Three lines of evidence support our conclusion that carbazole (**9**) formation represents the primary decay pathway for **1** in the absence of trapping agents.

(1) The yields of carbazole relative to both diphenylamine and the polymeric materials (see below) increase when photolysis of **2** is carried out in samples at high dilution. Table 1 shows the yields of carbazole and diphenylamine when **2** was photolyzed with room light in various solvents at various starting concentrations. In each case, decreasing starting material concentration results in a higher yield of carbazole. This is consistent with, but does not require, that both **8** and the polymeric materials be derived from accumulated photoproducts.

(2) The decay rate of the diphenylnitrenium ion shows clean first-order kinetics, and the rate constant does not vary significantly with solvent. This was established by LFP experiments, wherein diphenylnitrenium ion was generated by pulsed laser (355 nm, 20−40 mJ/pulse, 4−8 ns) photolysis of **2** in CH_3CN, toluene, and CH_2Cl_2. The decay of **1** was measured at its 440 nm absorption maximum, and the rate constants were determined to be $(7.7 \pm 1.4) \times 10^5$ s^{-1} in each of these solvents. The origin of diphenylamine through H atom (or hydride) abstraction from the solvent would require that each of these solvents react at equal rates, or more precisely, that any change in H atom transfer rates would be balanced by a commensurate change in cyclization rate. Such a mechanism is highly improbable. We also note that the clean first-order kinetics observed in these experiments are also inconsistent with the polymeric materials forming directly from coupling of two nitrenium ions. It should also be noted that the LFP experiments are carried out under conditions where accumulation of the photoproducts is expected to be negligible.

(3) Likewise, the decay rate constant shows no significant variation with the concentration of **2**. The decay rate constants measured over the concentration range of 15−240 μM and show variation that is indistinguishable from the experimental uncertainty.

The formation of carbazole from diphenylnitrenium ion formally requires the loss of one aryl proton and the net

(25) Cramer, C. J.; Falvey, D. E. *Tetrahedron Lett.* **1997**, *38*, 1515−1518.
(26) McIlroy, S.; Falvey, D. E. *J. Am. Chem. Soc.* **2001**, *123*, 11329−11320.

SCHEME 2. Nazarov-Type Cyclization of Diphenylnitrenium Ion to Carbazole

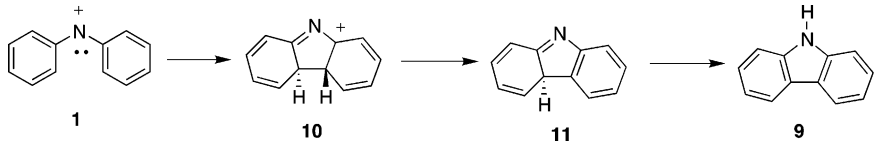

migration of one proton from the phenyl ring to the nitrogen. One possible mechanism for this process would an electrocyclization pathway, analogous to the Nazarov cyclization as shown in Scheme 2. The initial ring closure would form the protonated carbazole tautomer **10**. Conversion of this intermediate into stable products would require a deprotonation to give the carbazole tautomer **11** followed by a net 1,7 proton shift to give the observed product. Although the experiments and calculations described below cause us to favor a modification of this mechanism, Scheme 2 serves as a useful starting point for these discussions. This is because Scheme 2 identifies two limiting intermediates, **10** and **11**, that should be considered in light of any data.

To characterize the primary decay processes, we undertook more detailed LFP experiments on **2**, aimed at detecting the possible intermediates in this process. Figure 1 shows transient UV−vis spectra taken various times following pulsed laser photolysis (355 nm, 20 mJ, 4−8 ns) of **2** in toluene. As previously reported,[11] nitrenium ion **1** is formed concurrently with the excitation pulse and can be detected through its strong signals at 440 and 660 nm. The decay of these signals is accompanied by a first-order growth of a new species with $\lambda_{max} = 340$ nm. The new intermediate lives for ca. 15 μs. Similar behavior was observed in both CH_2Cl_2 and CH_3CN.

Following Scheme 2, the carrier for this 340 nm signal could be either the initial cyclization product **10** or the carbazole tautomer **11**. The former species decays through loss of a proton, a reaction that would be accelerated by the addition of base and slowed by addition of a strong acid. The latter species decays by a formal proton shift, a reaction that could be catalyzed by either an acid or a base. Two observations cause us to assign the signal to **11**. First, the decay rate of the observed species is accelerated both by added acid as well as added base. Specifically, we find that addition of 48% aqueous $HClO_4$ quenches the 340 nm signal with a rate constant of 8.2 10^8 M^{-1} s^{-1}. Likewise, addition of 1,3,5-collidine as a base,

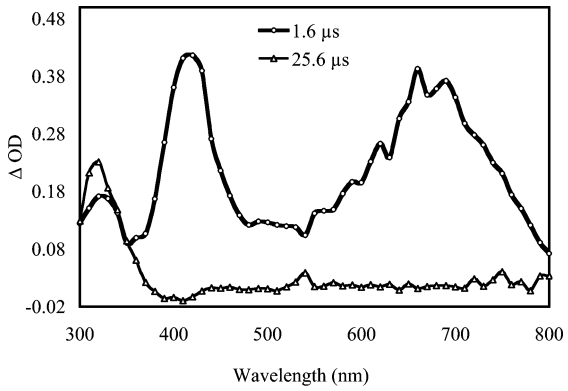

FIGURE 1. Transient UV−vis absorption spectra derived from pulsed photolysis of **2** in toluene.

TABLE 2. Significant UV−vis Absorption Bands (in nm) and Oscillator Strengths (i parentheses) Predicted for 1, 10, and 11 Compared to Assignments from LFP Experiments

method	1	10	11
TD-DFT	645 (0.14)	449 (0.22)	373 (0.16)
ZINDO	679 (0.26)	455 (0.33)	365 (0.28)
expt	660	n.d.	340

in concentrations too low to intercept significant fractions of **1**, also quenches this new intermediate with a rate constant of 7 $\times$ 10^8 $M^{-1}s^{-1}$.

Further verification of the assignment comes from theoretical calculations. Density functional theory (B3LYP/6-31G(d,p)) was used to optimized geometries for **10** and **11**. Similar calculations on **1** have been previously reported. From these geometries, UV−vis absorption bands were computed using both time-dependent density functional theory (TD-DFT)[27] as well as the semiempirical ZINDO method.[28] The presumably more accurate B3LYP geometries were used in the ZINDO calculations. The predicted UV−vis signals are shown in Table 2. In general, good agreement between the two computational predictions and the experimental values was observed. In particular, we note that both TD-DFT and ZINDO predictions are more consistent with the assignment of the 340 nm intermediate to **11**.

The electocyclization pathway was further examined by modeling the transition state leading to **10**. With the (B3LYP/6-31G(d,p) structures for **1** and **10**, the transition state for the reaction was located by means of the Berny algorithm at the AM1 level and then reoptimized at the DFT level. Analytic vibrational frequency calculations confirmed that structures **1** and **10** (Figure 2) are local minima, having no imaginary frequencies and that the transition state structure (**12**) is a saddle point, having a single imaginary frequency. In the absence of solvation, the conversion of **1** to **10** is predicted to be endothermic by ca. 13 kcal/mol, having a barrier of 16.6 kcal/mol. On the other hand, when the structures were reoptimized using a polarized-continuum solvation model, the reaction is predicted to be ca. 7 kcal/mol endothermic, with a barrier of 10 kcal/mol. The energies of **1**, **10**, and **12** are listed in Table 3, along with some selected geometric parameters, including C−N−C bond angle and the distance between the two carbons that become covalently attached in **10**. By these measures, product **10** is very similar in geometry to the transition state.

Given that the neutral intermediate **11** is observed to appear immediately following the decay of the nitrenium ion and that formation of **10** is likely to be endothermic with a significant barrier, it occurred to us that **11** could

(27) Marques, M. A. L.; Gross, E. K. U. *Annu. Rev. Phys. Chem.* **2004**, *55*, 427−455.

(28) Zerner, M. C. In *Reviews in Computational Chemistry*; Boyd, D. B., Lipkowitz, K. B., Eds.; VCH: New York, 1991; Vol. 2; pp 313−366.

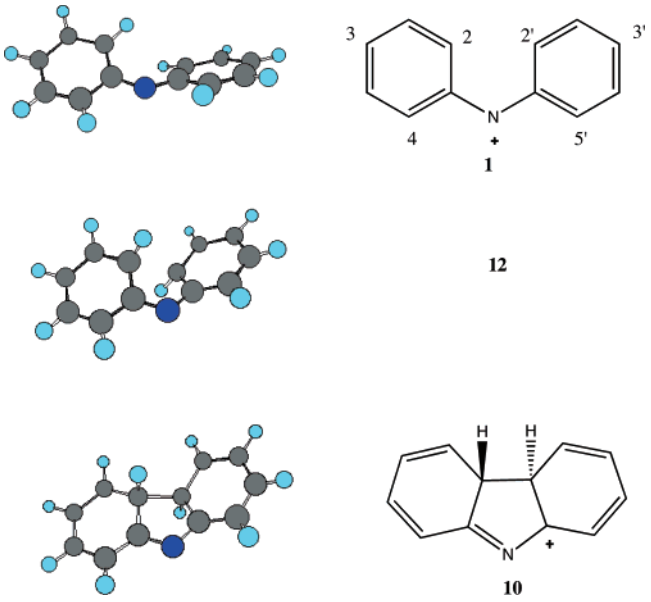

FIGURE 2. Calculated (B3LYP/6-31G(d,p) geometries for the conversion of **1** to **10**.

TABLE 3. Energies and Geometric Parameters for Intermediates and the Transition State in the Conversion of 1 to 10

structure	$<C_1NC_{1'}$ (deg)	$R(C_2-C_{2'})$ (Å)	$<H_2C_2C_{2'}H_{2'}$ (deg)	E (hartrees)
1	126.5	3.077	−97.0	−517.8558
12 (TS)	109.3	2.037	−165.7	−517.8325
10	107.5	1.621	−166.3	−517.8450

SCHEME 3. Concerted Proton Transfer/ Cyclization Mechanism

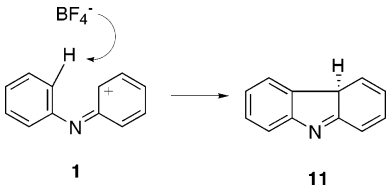

form through a concerted process**.** Therefore, we considered a pathway whereby the cyclization step is coupled to the proton loss (Scheme 3).

The acidity of structure **10** is not known, but the lack of aromaticity in any of the rings implies that it would be considerable. We can estimate its acidity (pK_{10}) using the thermodynamic cycle indicated in Figure 3. The latter relates pK_{10} to the acidity of carbazole (pK_9) and the free energy changes converting carbazole to its tautomer **11** (ΔG_9) and *N*-protonated carbazole (**9H**$^+$) to its isomer **10** (ΔG_{10}). Values of $\Delta G_9 = 28$ kcal/mol and $\Delta G_{10} = 46$ kcal/mol were obtained from AM1 calculations, assuming that zero-point vibrational energies, entropy changes, as well as solvation differences for these reactions to be negligible. From the studies of Chen et al.[29] we obtain $pK_9 = -6$. These values are applied to eq 1 to estimate the pK_a of **10** to be −19. This value is certainly consistent with intuitive expectation that deprotonation of **10** should be

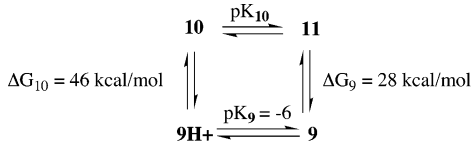

FIGURE 3. Thermodynamic cycle used to estimate the acidity of hypothetical intermediate **10**.

especially facile. Moreover, it suggests that **10** might not exist as a discrete intermediate, but that proton transfer to the counterion and/or the solvent would be concerted with its formation.

$$pK_{10} = pK_9 + \frac{\Delta G_9 - \Delta G_{10}}{2.3RT} \qquad (1)$$

Bessiere[30] estimates the pK_a of HBF_4 as −4.9. Even allowing for some rather large (>16 kcal/mol) discrepancies in the estimation of $\Delta G_9 - \Delta G_{10}$, proton transfer to the counterion should be highly favored. In fact, the pK_a's of both HBF_4 and **9H**$^+$ were determined in polar protic media, which would favor the formation of ions. It is expected in the aprotic media employed here both that the favorability of proton transfer from **10** to the BF_4^- counterion is underestimated as a result. Thus, we suggest that the mechanism for carbazole formation in solution is the cyclization reaction coupled to a transfer of the C2 proton to the BF_4^- counterion as shown in Scheme 3. We note that proton transfer to the 2,4,6-trimethylpyridine leaving group is also possible. Further computational and experimental studies aimed at determining the degree of proton transfer in the transition state would certainly be interesting but beyond the scope of the present investigation.

B. Secondary Products. We next turned our attention to the formation of diphenylamine (**8**) from photolysis of **2**. The former results from a net two-electron reduction of nitrenium ion **1**. However, the source of the reducing equivalents has never been elucidated. The possibility that they might derive from the solvent (via either H atom or hydride transfer) seems unlikely, given the invariance of the decay rate with the different solvents employed. Therefore, we considered the possibility that this might be derived from a reaction of **1** with accumulated photoproducts.

To identify possible accumulated photoproducts, the photolyzates from **2** were analyzed in more detail. In particular we scaled up the reaction and carried out chromatographic separations on the mixture. These experiments reveal that, in addition to the major photoproducts **8** and **9**, two dimeric species (**13** and **14**) were also formed (Figure 4). Product **13** clearly derives from coupling between a diphenylnitrenium ion and carbazole. Interestingly, this adduct forms from addition of the nitrogen of carbazole to the 4-position of the nitrenium ions arylsubstituent. This adduct was distinguished from its isomers by the number of signals in the ^{13}C NMR spectrum. Assuming rapid rotation about single bonds, product **13** is predicted to give 14 unique signals, which is exactly what is observed. We also considered the possible coupling of the nitrenium center with the 3-position on carbazole, which would have 16 unique carbons.

(29) Chen, H. J.; Hakka, L. E.; Hinman, R. L.; Kresge, A. J.; Whipple, E. B. *J. Am. Chem. Soc.* **1971**, *93*, 5102−5107.

(30) Bessiere, J. *Anal. Chim. Acta* **1970**, *52*, 55−63.

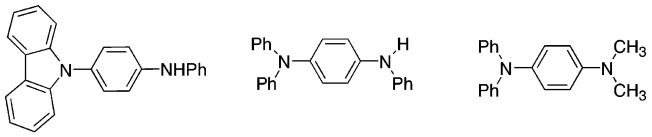

13 **14** **15**

FIGURE 4. Structures of adducts obtained from photolysis of **2** in the presence of carbazole yielding **13**, diphenylamine yielding **14**, and *N*,*N*-dimethylaniline yielding **15**.

TABLE 4. Yields of Diphenylamine (8) and Adducts 13 and 14 from Photolysis of 2 in CH_3CN with Varying Concentrations of Added Carbazole

	yield (μM)		
carbazole (μM)	**8**	**13**	**14**
266	52	110	26
1700	78	320	tr
4800	99	830	tr

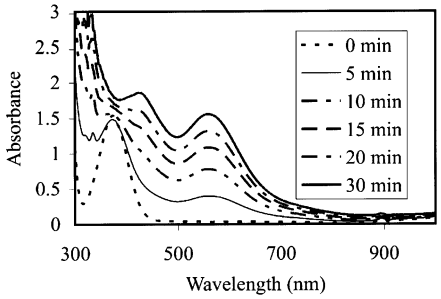

FIGURE 5. Steady-state UV−vis absorption spectra taken at various times following photolysis of **2** in a CH_3CN solution.

A structure derived from coupling the 4-position of the nitrenium ion fragment with the 3- or 1-positions of carbazole would each give 20 unique signals.

The other dimeric species, **14**, derives from the coupling of a nitrenium ion with diphenylamine. This was confirmed by carrying out photolyses with added diphenylamine. Under these conditions **14** is the major product. As with **13**, this species can be distinguished from its isomers on the basis of the number of ^{13}C NMR peaks. For compound **14**, 12 unique signals are predicted and 12 are observed.

Carbazole is postulated to be the primary photoproduct. In that case, diphenylamine and **13** would be derived from secondary reactions of **1** with this product. To test this point, we generated the former in the presence of excess carbazole and examined product distributions by GC. As shown in Table 4, the yields of both the adduct **13** and **8** increase as the carbazole concentration is raised.

The structures of the two minor products suggested that the remaining materials might be derived from higher order addition reactions creating mixed oligomers of carbazole and diphenylamine. Two observations support this. Figure 5 shows changes in the UV−vis spectra resulting from photolysis of **2** in CH_3CN with a handheld shortwave UV lamp. The product absorption band at 570 nm signals the formation of an extended π-system. Similar visible absorption bands are characteristic of both poly(diphenylamine) and poly(3,6-carbazole).[31]

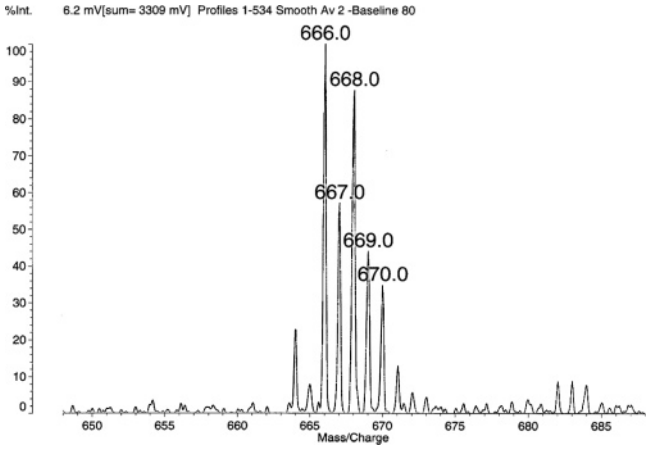

FIGURE 6. A portion of the MALDI-TOF-MS derived from photolysis of **1** in CH_3CN.

TABLE 5. Trapping Rate Constants and Product Yields for the Reaction of Various Arenes with 1

arene	k_{trap} (M^{-1} s^{-1})	**8** (%)	adduct (%)	LFP signal (nm)
$PhN(CH_3)_2$	7.3×10^9	57	**15** (17)	480
Ph_2NH	1.3×10^{10}	n.d.	**14** (16)	690
Ph_3N	7.0×10^9	76	n.d.	360, 560
1,4-DMB	2.0×10^9	39	n.d.	480
Carbazole	1.3×10^9	51	**13** (24)	680

The formation of these oligomeric species is further confirmed by MALDI-TOF mass spectra of the reaction products. Figure 6 shows a portion of the latter in the region corresponding to tetramers having varying amounts of carbazole and diphenylamine. Similar sets of peaks are detected at 833 and 1000 amu, corresponding to pentamers and hexamers, respectively.

C. Reactions of 1 with Electron Rich Aromatics. The observations of the oligomers from the nontrap photolysis lead us to explore the reactions of diphenylnitrenium ion with diphenylamine and carbazole, as well as with several related arylamines. In this study, we focused our attention on arene traps having low oxidation potentials (E_{ox} < +1.4 V vs SCE). Table 5 shows rate constants for the reaction of **1** with these traps. These rate constants were determined from LFP experiments wherein **1** was generated from photolysis of **2** and the pseudo-first-order decay rate constant, k_{obs}, of **1** was determined with various concentrations of trap. These data were analyzed using eq 2, and in each case a good linear correlation was obtained. As is apparent from Table 5, these traps react with diphenylnitrenium ion at near the diffusion limit of CH_3CN (1.9×10^{10} M^{-1} s^{-1}).

$$k_{obs} = k_0 + k_{trap}[trap] \quad (2)$$

Each of the traps in Table 5 react with diphenylnitrenium ion via an electron-transfer reaction. Figure 7 shows transient absorption spectra acquired following pulsed laser photolysis of **2** in the presence of *N*,*N*,*N*-triphenylamine, *N*,*N*-dimethylaniline, 1,4-dimethoxybenzene, *N*,*N*-diphenylamine, and carbazole. In each case, following the decay of nitrenium ion **1**, we detect radical

(31) Wen, T.-C.; Chen, J.-B.; Gopalan, A. *Mater. Lett.* **2002**, *57*, 280−290.

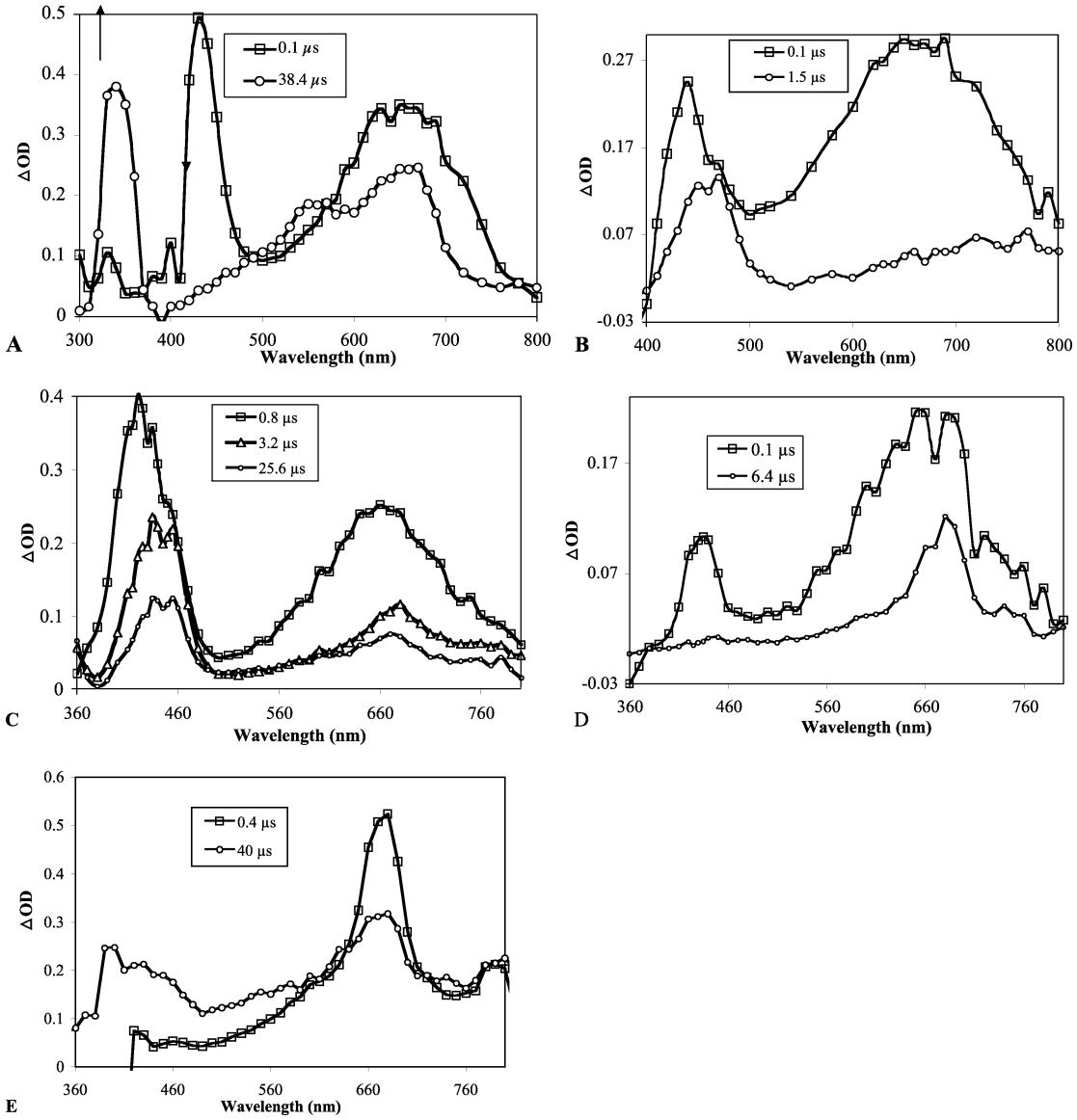

FIGURE 7. Transient absorption spectra from LFP of **2** in CH_3CN with (a) 0.15 mM *N*,*N*,*N*-triphenylamine, (b) 0.59 *N*,*N*-dimethylaniline, (c) 0.82 mM 1,4-dimethoxybenzene, (d) 0.6 mM *N*,*N*-diphenylamine, and (e) 3.0 mM carbazole with HBF_4.

ion intermediates resulting from electron transfer.[32] Specifically, radical cations for *N*,*N*,*N*-triphenylamine (λ_{max} = 373 and 560 nm), *N*,*N*-dimethylaniline (λ_{max} = 440 nm), 1,4-dimethoxybenzene (λ_{max} = 410 and 425 nm), and *N*,*N*-diphenylamine (λ_{max} = 690 nm) are detected, along with a weaker, broad absorption for diphenylamine neutral radical, which has a maxima near 650 nm.[33] In the case of carbazole the spectra are complicated in CH_3CN as a result of the acidity of both the carbazole cation radical (pK_a = 1.5) and the diphenylamine cation radical (pK_a = 2.5).[34] However, when experiments were carried out with added HBF_4, the well-resolved spectrum of the diphenylamine cation radical (λ_{max} = 680 nm) was observed. The corresponding carbazole radical was not detected, but its relatively weak absorption (610 nm)[35] may be obscured by the stronger signal for diphenylamine cation radical.

The stable products from each of these reactions was analyzed. Aside from the adducts listed in Table 5, significant amounts of the polymers were also formed. In the case of diphenylamine, it was impractical to assess the yield of any additional diphenylamine, which would have corresponded to a relatively small increase in the signal due to unconverted trap. In the case of *N*,*N*,*N*-triphenylamine and 1,4-dimethoxybenzene, no adducts formed in sufficient yields to allow for characterization. In the case of *N*,*N*-dimethylaniline, an adduct was isolated. This compound is derived from coupling the 4-position of the *N*,*N*-dimethylaniline with the nitrogen from diphenylnitrenium ion as seen in Figure 4.

On the basis of these LFP and product analysis experiments, we provide Scheme 4, which is consistent with all current results. Nitrenium ion **1** forms carbazole

(32) Shida, T. *Electronic Absorption Spectra of Radical Ions*; Elsevier: Amsterdam, 1988.
(33) Leyva, E.; Platz, M. S.; Niu, B.; Wirz, J. *J. Phys. Chem.* **1987**, *91*, 2293−2298.
(34) Bordwell, F. G.; Zhang, X.-M.; Cheng, J.-P. *J. Org. Chem.* **1993**, *58*, 6410−6416.
(35) G. A. DiLabio; Litwinienko, G.; Lin, S.; Pratt, D. A.; Ingold, K. U. *J. Phys. Chem. A* **2002**, *106*, 11719−11725.

SCHEME 4. Dimerization and Oligomerization of Intermediates from Diphenylnitrenium Ion

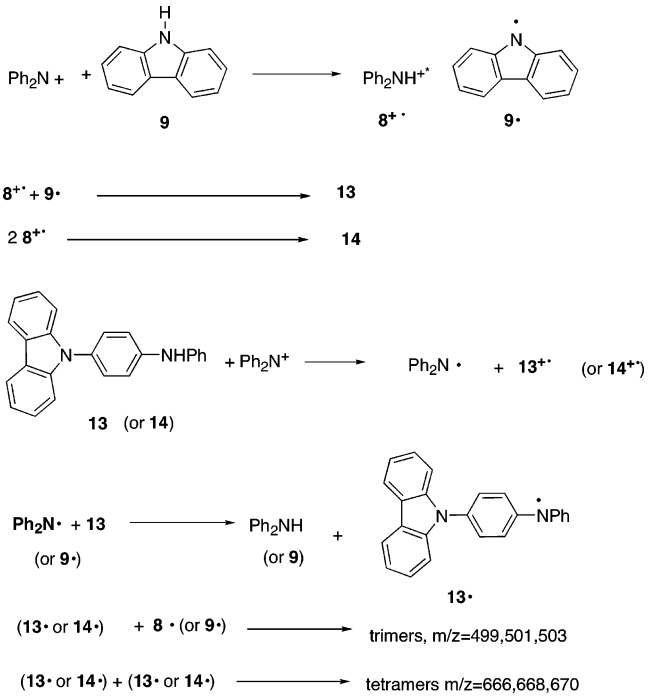

in the absence of traps. As the carbazole accumulates, **1** reacts with this product via a net H atom abstraction (we suggest that this is a stepwise electron transfer/proton-transfer process, but the current data are not conclusive on this point). Coupling of the 9-carbazolyl radical with the diphenylamine cation radical forms the dimeric product **13**. The cation radical of **8** can then either couple with another cation radical of **8** to form **14** or abstract an additional electron from the various photoproducts to form diphenylamine. Likewise, carbazolyl radical (**9**•) can also be expected to oxidize (or abstract a H atom from) any of the oligomeric species. Subsequent oxidation of the dimeric products by **1** is followed by coupling reactions creating trimers and tetramers. Higher order oligomers are generated by analogous oxidation/coupling processes. Thus, each nitrenium ion is capable of oxidizing two oligomers, which in turn can couple to form larger species. The present studies do not permit a definitive assignment of the structures of any of the oligomers larger than the dimers **13** and **14** because of the complexity of these mixtures. However, the similarity of the UV−vis spectrum to that obtained from poly(diphenylamine) suggests that their structures are analogous.

Earlier mechanistic studies of oxidative aniline polymerization considered two mechanisms. The first postulated chain elongation via coupling of a nitrenium ion with a aniline derivative.[8,36] More recent work suggests that the chain growth occurs through coupling of two aniline (or aniline oligomer) cation radicals and that arylnitrenium ions are not involved.[37−39] While the current work does not directly address this issue, it is interesting to note that the two mechanisms are really not all that distinct. Generalizing from Scheme 4, it would seem that any encounter between a nitrenium ion and an aniline derivative (or oligomer) would produce the same intermediates derived from the radical mechanism. Further investigations into the specific intermediates in PANI formation are currently being pursued.

Conclusions

The experiments described here further develop the view of diphenylnitrenium ion chemistry. First, it is clear that the primary decay pathway (in solution) for diphenylnitrenium ion is a concerted electrocyclization/deprotonation reaction that provides carbazole via its H-4a tautomer (**11**). The latter can be detected in LFP experiments. Laser flash photolysis experiments and product analysis show that with relatively easily oxidized arenes the reaction with diphenylnitrenium ion goes through an initial electron transfer rather than direct formation of a σ complex. The electron-transfer reactions lead to diphenylamine and, in many cases, oligomeric products derived from oxidation and coupling reactions. This appears to be the first direct observation of one-electron-transfer reactions from a singlet nitrenium ion.

Experimental Section.

Calculations. All geometry optimizations and vibrational frequency calculations were carried out using the Gaussian 03 suite of programs.[40] The values in Tables 2 and 3, as well as Figure 2, were calculated using density functional theory and in particular the hybrid B3LYP functional, composed of Becke's B3 three-parameter gradient-corrected exchange functional[41,42] with the LYP correlation functional of Lee, Yang, and Parr[43] as originally described by Stevens et al.[44] Unless noted, the 6-31G(d,p) basis set was used for these calculations.[45] The thermochemical analysis in Figure 3 used AM1-derived[46] energies for **9**, **9H**$^+$, **10**, and **11**.

Laser Flash Photolysis Studies. Laser flash photolysis experiments were performed at 298 K using a Nd(YAG) laser. Second, third, and fourth harmonic generator crystals were used to create output wavelengths at 355 and 266 nm. The UV−vis light source was produced by a CW 350 W Xe arc lamp. The solution to be photolyzed, unless otherwise noted,

(36) Wei, Y.; Tang, X.; Sun, Y. *J. Polym. Sci., Part A*: *Chem.* **1989**, *27*, 2385−2396.
(37) Ding, Y.; Padias, A. B.; H. K. Hall, J. *J. Polym. Sci., Part A*: *Polym. Chem.* **1999**, *37*, 2569−2579.
(38) Lux, F. *Polym. Rev.* **1995**, *35*, 2915.
(39) Holze, R. *Collect. Czech. Chem. Commun.* **2000**, *65*, 899−923.
(40) Frisch, M. J.; Trucks, G. W.; Schlegel, H. B.; Scuseria, G. E.; Robb, M. A.; Cheeseman, J. R.; J. A. Montgomery, J.; Vreven, T.; Kudin, K. N.; Burant, J. C.; Millam, J. M.; Iyengar, S. S.; Tomasi, J.; Barone, V.; Mennucci, B.; Cossi, M.; Scalmani, G.; Rega, N.; Petersson, G. A.; Nakatsuji, H.; Hada, M.; Ehara, M.; Toyota, K.; Fukuda, R.; Hasegawa, J.; Ishida, M.; Nakajima, T.; Honda, Y.; Kitao, O.; Nakai, H.; Klene, M.; Li, X.; Knox, J. E.; Hratchian, H. P.; Cross, J. B.; Adamo, C.; Jaramillo, J.; Gomperts, R.; Stratmann, R. E.; Yazyev, O.; Austin, A. J.; Cammi, R.; Pomelli, C.; Ochterski, J. W.; Ayala, P. Y.; Morokuma, K.; Voth, G. A.; Salvador, P.; Dannenberg, J. J.; Zakrzewski, V. G.; Dapprich, S.; Daniels, A. D.; Strain, M. C.; Farkas, O.; Malick, D. K.; Rabuck, A. D.; Raghavachari, K.; Foresman, J. B.; Ortiz, J. V.; Cui, Q.; Baboul, A. G.; Clifford, S.; Cioslowski, J.; Stefanov, B. B.; Liu, G.; Liashenko, A.; Piskorz, P.; Komaromi, I.; Martin, R. L.; Fox, D. J.; Keith, T.; Al-Laham, M. A.; Peng, C. Y.; Nanayakkara, A.; Challacombe, M.; Gill, P. M. W.; Johnson, B.; Chen, W.; Wong, M. W.; Gonzalez, C.; Pople, J. A. *Gaussian03*, Revision B.03.; Gaussian, Inc.: Pittsburgh, PA, 2003.
(41) Becke, A. D. *Phys. Rev. A* **1988**, *38*, 3098−3100.
(42) Becke, A. D. *J. Chem. Phys.* **1993**, *98*, 5648−5652.
(43) Lee, C.; Yang, W.; Parr, R. G. *Phys. Rev. B* **1988**, *37*, 785−789.
(44) Stevens, P. J.; Devlin, F. J.; Chabalowski, C. F.; Frisch, M. J. *J. Phys. Chem.* **1994**, *98*, 11632−11627.
(45) Hehre, W. J.; Radom, L.; Schleyer, P. v. R.; Pople, J. A. *Ab Initio Molecular Orbital Theory*; Wiley: New York, 1986.
(46) Dewar, M. J. S.; Zoebisch, E. G.; Healy, E. F.; Stewart, J. J. P. *J. Am. Chem. Soc.* **1985**, *107*, 3902−3909.

was prepared in an anhydrous N_2 purged flow cell equipped with a magnetic stir-bar. Once prepared the solution was purged for 10 min with N_2 and then sealed with a rubber septum.

Kinetic studies performed on diphenylnitrenium ion used stock solutions of 20 mg of 1-(*N*,*N*-diphenylamino)-2,4,6-trimethylpyridinium tetrafluoroborate in 60 mL of solvent, the solvent being CH_2Cl_2, toluene, or CH_3CN. A 3 mL portion of the stock solution was taken via syringe and placed in a N_2 purged quartz cuvette. The cuvette remains under N_2 pressure during the LFP experiments. At least five different concentrations, ranging from 0 to 2.2 mM, of each quencher were obtained through the addition of pure quencher via syringe to determine the rate constants shown in Table 5.

MALDI-TOF-MS. Compound **2** (0.0806 g) was dissolved in 10 mL of dry CH_3CN (0.2149 mmol; 21.49 mM), and then the solution was purged under N_2 for 15 min. A 1 mL portion of the solution was removed as a dark standard. The remaining solution was photolyzed with a Xe lamp for 3 h. For the matrix, 0.2013 g of 2,5-dihydroxybenzoic acid was dissolved in 10 mL CH_3CN. Next, 0.5 mL of sample and 0.5 mL of matrix were mixed in a vial, and then 1 μL of acetic acid was added. The sample plate was spotted with 1 μL of matrix alone and allowed to air-dry. Then 1 μL of sample and matrix solution was co-spotted and allowed to air-dry. The samples were then analyzed using a MALDI-TOF-MS instrument.

Acknowledgment. This work was supported by the Chemistry Division of the National Science Foundation. We thank Mr. Art Winter for assistance with the calculations.

Supporting Information Available: ^{1}H NMR and ^{13}C NMR spectra for adducts **13**−**15**; Cartesian coordinates from DFT calculations on **1** and **10**−**12**; and detailed descriptions of preparative photolysis reactions generating compounds **13**−**15**. This material is available free of charge via the Internet at http://pubs.acs.org.

JO050598Z